Elias A. Zerhouni, MD • David M. Parish, MD • Walter J. Rogers, PhD • Andrew Yang, MD • Edward P. Shapiro, MD

Human Heart: Tagging with MR Imaging—A Method for Noninvasive Assessment of Myocardial Motion[1]

Specified regions of the myocardium can be labeled in magnetic resonance (MR) imaging to serve as markers during contraction. The technique is based on locally perturbing the magnetization of the myocardium with selective radio-frequency (RF) saturation of multiple, thin tag planes during diastole followed by conventional, orthogonal-plane imaging during systole. The technique was implemented on a 0.38-T imager and tested on phantoms and volunteers. In humans, tags could be seen 60-450 msec after RF saturation, thus permitting sampling of the entire contractile phase of the cardiac cycle. Tagged regions appear as hypointense stripes, and their patterns of displacement reflect intervening cardiac motion. In addition to simple translation and rotation, complex motions such as cardiac twist can be demonstrated. The effects of RF pulse angle, relaxation times, and heart rate on depiction of the tagged regions are discussed.

Index terms: Heart, function, 51.1214 • Heart, MR studies, 51.1214 • Magnetic resonance (MR), physics • Myocardium, MR studies, 511.1214

Radiology 1988; 169:59-63

INVESTIGATIONS of the biomechanical properties of normal and abnormal heart muscle are fundamental to understanding the effects of cardiovascular disease and therapeutic interventions on ventricular performance. Noninvasive measurements of wall motion and thickening during contraction are essential to such an understanding and have been the subject of extensive research with radioisotope and echocardiographic imaging techniques (1-3). However, despite the increasing sophistication of imaging technology, an impediment to the analysis of myocardial dynamics remains the inability to ensure that the same portion of the ventricular myocardium is imaged throughout the cardiac cycle. Indeed, all current tomographic imaging methods, including magnetic resonance (MR) imaging and cine computed tomography, demonstrate a fixed section of space through which the myocardium moves during the cardiac cycle. Therefore, systolic and diastolic images sample different segments of the myocardium, leading to uncertainty in measurements of wall thickening and excursion (4). Metallic markers or sonomicrometers implanted in the myocardium have been used in animals and humans for research purposes, but these techniques cannot be applied clinically (5,6).

This report presents an MR imaging method based on tagging myocardial tissue with radio-frequency (RF) saturation before acquiring images. The technique can be used to label and track specific regions of the myocardium during contraction, thus enabling studies of motion with the equivalent of multiple, noninvasively generated markers.

MATERIALS AND METHODS

Theoretic Considerations

The essential element of the technique is the application, before imaging, of a selective RF pulse in the presence of linear magnetic-field gradients, thus perturbing the magnetization of protons in one or several tissue sections. The perturbed protons retain memory of the RF excitation for a time, mainly dependent on the longitudinal relaxation time, T1, of the tissue of interest. If, before full recovery of magnetization in the RF-perturbed area, an MR image of the tissue is obtained in a plane orthogonal to the tagged plane, there will be a signal difference between the tagged and nontagged regions, caused by their disparate degrees of saturation. Motion occurring between tagging and imaging time will be reflected by displacement and distortion of the tagged regions, which will appear as stripes of different signal intensity. The location, number, thickness, and signal intensity of these tagged regions can be changed by modulating the RF pulse angle and the strength and direction of the magnetic-field gradients.

The depiction of the tags and therefore the time during which cardiac motion can be monitored depends on the signal difference (SD) generated between tagged and nontagged regions. Understanding the effects of the variables affecting such signal difference is thus critical to the method.

Assuming that the repetition time (TR) is much greater than T2, an acceptable approximation of the signal intensity of the nontagged regions for a standard spin-echo imaging sequence is given by

$$SI(\text{nontagged}) = M(1 - \exp^{-TR/T1}) \times (\exp^{-TE/T2}), \quad (1)$$

where SI is signal intensity, M is proton density of the myocardium, T1 and T2 are its longitudinal and transverse magnetic relaxation times, respectively, TR is the repetition time of the imaging sequence and TE (echo time) is the time between the first RF pulse of the imaging sequence and the recording of the spin echo. TR is equal to the duration of the cardiac cycle, since all studies are electrocardiographically gated.

The signal intensity of the tagged regions can be approximated by

$$SI(\text{tagged}) = M[1 + (\cos\Phi - 1) \times \exp(^{-TD/T1}) - \cos\Phi \exp(^{-TR/T1})], \quad (2)$$

[1] From the Russell H. Morgan Department of Radiology and Radiological Science (E.A.Z., A.Y.) and the Division of Cardiology of the Department of Medicine (W.J.R., E.P.S.), The Johns Hopkins Medical Institutions, Baltimore, and Resonex, Inc, Sunnyvale, Calif (D.M.P.). Received January 26, 1988; revision requested March 23; revision received May 9; accepted June 13. Supported in part by Resonex, Inc. **Address reprint requests to** E.A.Z., MRI Division, The Johns Hopkins Hospital, Baltimore, MD 21205.

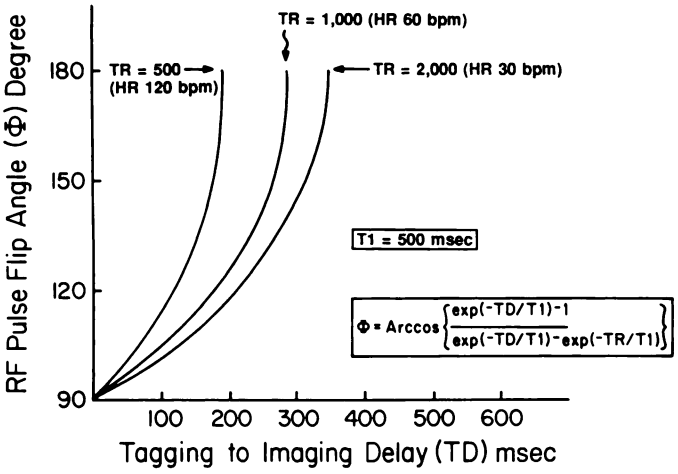

1.

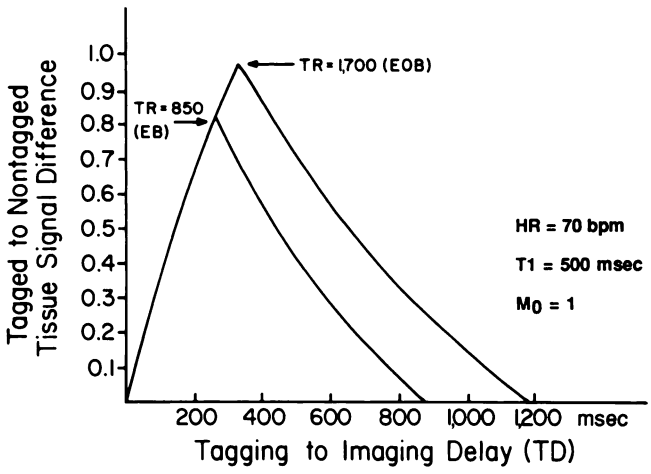

2.

Figures 1, 2. **(1)** Optimal RF pulse angle to achieve maximum SD between tagged and nontagged tissues for a given TD between tagging and imaging is given for a T1 of 500 msec, representative of the T1 of myocardium at a middle field strength of 0.3–0.6 T. Maximum tracking times are achieved with 180° pulses. Lengthening TR by acquiring images every second or third beat can also increase tracking time. *HR* = heart rate in beats per minute (*bpm*). **(2)** SD between tagged and nontagged regions versus TD between tagging and imaging is graphed for a 180° RF tagging pulse and an average heart rate (*HR*) of 70 beats per minute (*bpm*), that is, an effective TR of 850 msec, assuming a T1 value of 500 msec for myocardium. SD increases to peak value when null magnetization in the tagged region is reached and decreases thereafter. SD can be made to persist for a longer time simply by acquiring data every other heartbeat, thus increasing effective TR. *EB* = every beat, *EOB* = every other beat.

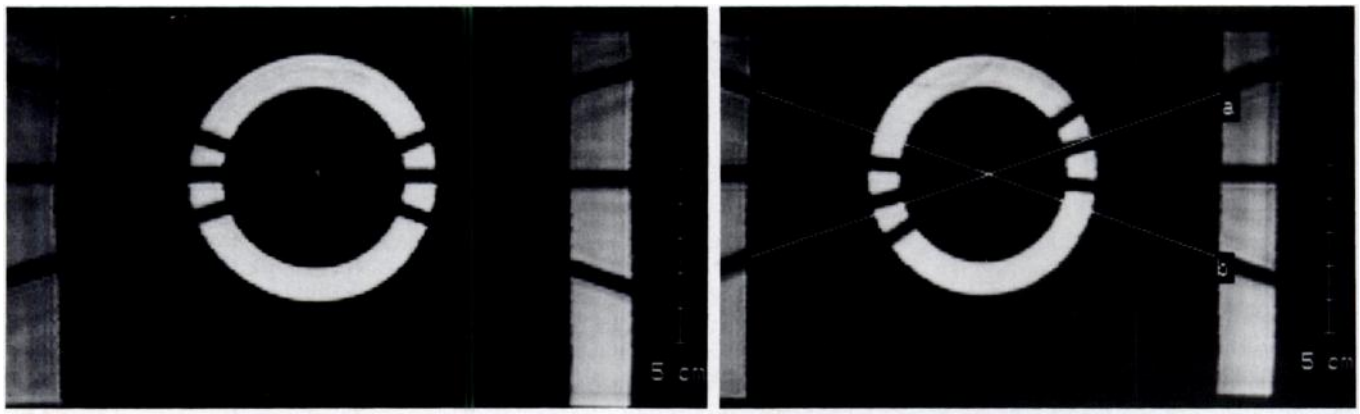

a. b.

Figure 3. **(a)** Phantom in stationary mode. Three radial tags were generated, and phantom was imaged 300 msec later. Tags are visible as dark stripes. Tags in cylindrical part of phantom are aligned with their counterparts in two slabs lateral to the cylinder. **(b)** Phantom in rotating motion. Note displacement of tags in the cylindrical part of phantom relative to their original location in stationary lateral slabs, thus showing amount of intervening motion between time of tagging and time of imaging.

where TD is the time delay between the tagging RF pulse and the first 90° pulse of the imaging sequence, and Φ is the flip angle of the magnetization vector achieved by the selective tagging RF pulse. Equation (2) also assumes that T2 is short relative to TD or TR.

Imaging has to be performed before equalization of signal intensity occurs between tagged and nontagged regions. The SD between the two regions is a function of TR, TD, T1, and flip angle. Some understanding of the relationships of each of these variables to depiction of the tags and to the time available for motion tracking with this technique is important. The computation of optimal flip angle for maximum tagged-to-nontagged tissue contrast for a given TD between tagging and imaging at various TR values and a T1 of 500 msec (an approximate value for T1 of myocardium at midfield strength) is graphed in Figure 1. By varying the flip angle from 90° to 180°, maximum contrast can be maintained to a maximum TD equal to 0.69 T1 for a TR of 4 × T1 or more. Since effective TR depends on heart rate, the maximum TD up to which maximum contrast can be achieved will vary somewhat from patient to patient, with tracking time being shorter with faster heart rates. For most of our experiments, a 180° saturation pulse was used to allow maximum tracking times.

For 180° saturation pulses, the signal-intensity behavior of the tagged tissues is identical to that on a conventional inversion-recovery sequence, thus reaching maximum contrast (assuming magnitude reconstruction) when longitudinal magnetization is null and with decreasing contrast before and after that time. Increasing tracking time at a given heart rate can be achieved by acquiring data at every other heartbeat (Fig 2).

Implementation

All experiments were performed on a whole-body, iron-core resistive MR imager (Rx 4000; Resonex, Sunnyvale, Calif) operating at 0.38 T. At such a field strength, the T1 relaxation time of myocardium is about 500 msec and is long enough for differential magnetization to persist through a large part of the cardiac cycle and allow adequate study of its contractile phase.

Machine software was modified to allow independent control of each element of the MR image-generation process. The

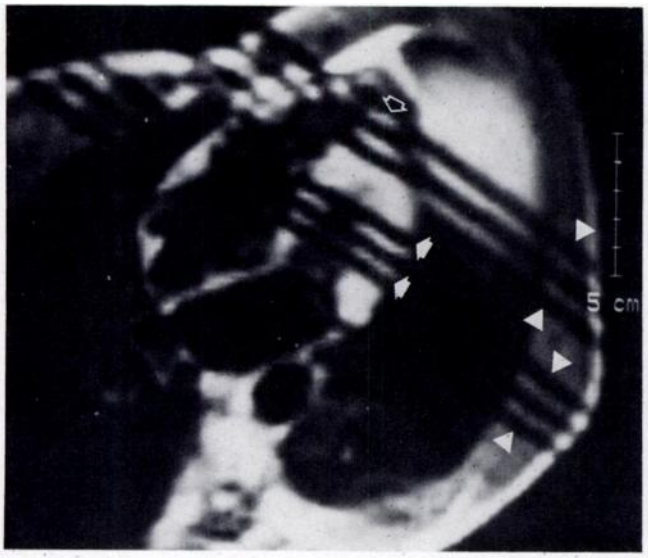

4.

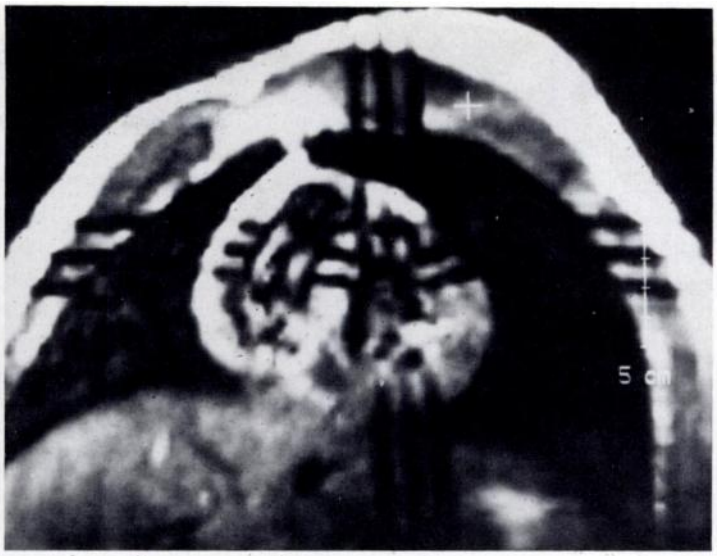

5.

Figures 4, 5. **(4)** Two triple-frequency, selective, 180° RF pulses were generated 12 msec apart at mid diastole in a plane perpendicular to the long axis of the heart. This separately tagged the base and apex with three 0.35-cm-thick parallel planes separated by 0.35 cm of nontagged tissue. The heart was then imaged 250 msec later at about mid systole in the long axis. Note the motion of the tagged regions relative to their original location, indicated by the set of dark lines in the thoracic wall structures (arrowheads). Group of tag lines at base (solid arrows) has moved toward the apex by 15 mm for the most basal line and by 10 mm for the most apical line. Degree of contraction of the muscle is recorded by decreased separation between tag lines at the base compared with that between the apical tags. Group of lines at apex (open arrow) demonstrates that most apical region of left ventricle has moved very little. This experiment demonstrates ability of the technique to identify and quantify the regional (base-versus-apex) motion patterns as well as intrinsic changes due to contraction (with tag-separation measurements). **(5)** Two orthogonal sets of three-lobed RF pulses imposed at diastole have imprinted a gridlike pattern on the myocardium. Imaging in the short axis of the left ventricle at early systole demonstrates intervening deformation and reorientation of the tag lines relative to their diastolic position, indicated by the chest wall tags. Tags in the subcutaneous and epicardial fat are not demonstrated, because of the shorter T1 relaxation time of fat.

critical features of the method are: completely arbitrary selection of orientation and thickness for each tagging and imaging section; independent prescription of each RF pulse, including flip angle, spectral width, and wave forms; arbitrary selection of TDs between each tagging or imaging section; and independent prescription of as many tagging and imaging sections as possible in the R-R interval. Hardware modifications were not necessary. To obtain a cross-sectional image of the displaced tagged regions within the heart, conventional multisection, spin-echo imaging was performed in a plane orthogonal to tagging planes after appropriate TDs. The original position of the tags can be deduced from their imprint on stationary structures such as the chest wall. The most efficient imaging scheme is to acquire multiple sections in the same R-R interval at different locations and TDs after tagging. Changing the order of acquisition of the sections on later sequences permits imaging of several planes at multiple phases of the cardiac cycle.

Experiments

Phantom studies.—For validation purposes, a series of experiments was performed on a phantom made of a hollow cylinder, 12 cm in diameter, filled with a gelatin mixture approximating the relaxation times of myocardium. With the drive mechanism of a Harvard injection pump, the cylinder could be rotated at speeds of 0.1, 0.2, 0.5, or 1 rotation per second. Stationary, rectangular plastic containers filled with the same gelatin were placed alongside the rotating phantom to serve as fixed points of reference. The phantom was first imaged when it was not moving, to evaluate linearity and definition of tags with varying imaging values (Fig 3a). A series of images of the phantom during rotation and at various TDs was then obtained to evaluate accuracy in determining angular displacements, with comparison of measured and expected values (Fig 3b).

Human studies.—Eight healthy volunteers ranging in age from 18 to 36 years with heart rates of 54–75 beats per minute were examined after informed consent was obtained. All studies were electrocardiographically synchronized, with the R wave of the QRS complex as trigger. Tagging, with 180° selective RF pulses, was performed 4 msec after the R wave. The time of end systole was determined by phonographic recording of the second heart sound. All tagging and imaging sections were prescribed on the basis of a series of preliminary axial and right anterior oblique views to determine the necessary angles and offset values. Images were acquired at different phases of the cardiac cycle 30–500 msec after tagging. Up to five spin-echo images per R-R interval were acquired in a multisection mode. The minimum intersequence delay was 57 msec. Most images were acquired with a matrix of 128 × 128 pixels, two signals averaged, a standard body coil with 30-cm field of view, and a two-dimensional Fourier transform method. In selected instances, a 256 × 256 pixel matrix or four signal averages were used. Total imaging time was 28–56 minutes, depending on the number of phase-encoding steps per image (128 or 256) and the number of signals averaged (two or four).

RESULTS

Multifrequency RF pulses capable of generating up to three simultaneous, parallel tagging planes were successfully implemented. Minimum achievable thickness of tagging planes was 0.35 cm. Minimum time per tagging section was 12 msec from the center of the tagging RF pulse to the center of the next tagging pulse.

Phantom measurements with a 128 × 128 matrix and a 23-cm field of view, that is, 1.8 × 1.8-mm pixels, demonstrated linearity of stationary tags. This was determined with linear regression analysis of the values of the x-y coordinates of a series of 15 points along the tag, measured at the center of the area of signal void representing the tags. A correlation coefficient of .99 was found, with a constant offset of 4 mm ± 2 between prescribed and measured values, probably due to a systematic inaccuracy in calibration. No significant

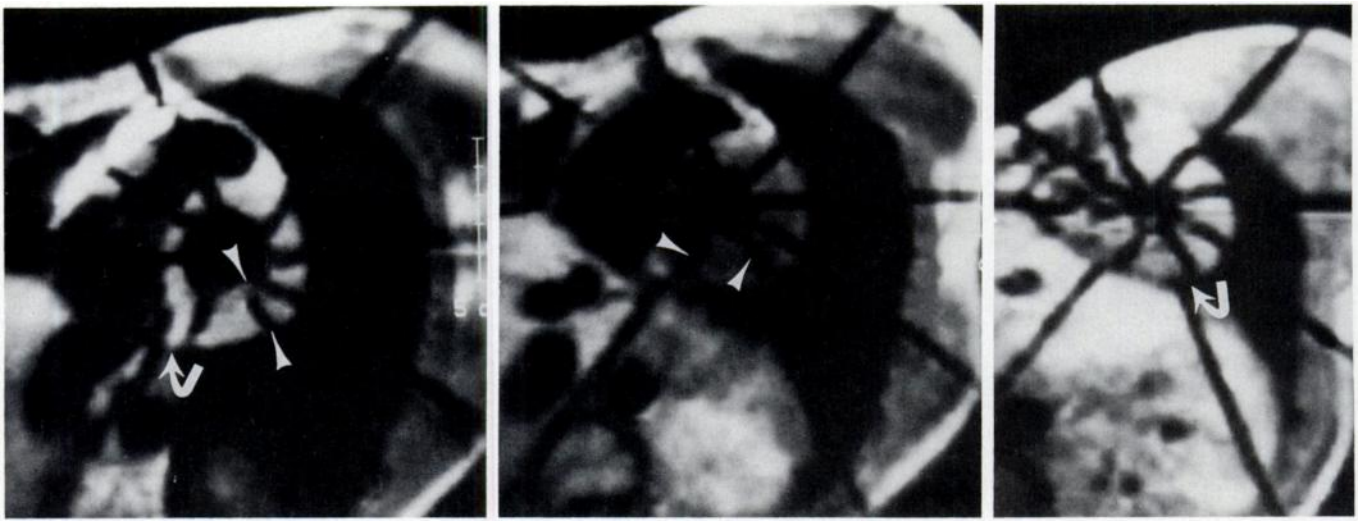

a. b. c.

Figure 6. Radially oriented tagging with imaging in the short axis of the heart is demonstrated. Four radially oriented tagging planes are generated at or near diastole followed by multisection imaging in short axis with acquisitions of five different anatomic sections in a single R-R interval, 30–450 msec after RF tagging. This tagging scheme is well suited to tracking global, regional, and intrinsic rotational motion around long axis of the heart. Three images obtained in early systole at base **(a),** middle **(b),** and apex **(c)** of the heart show global counterclockwise rotation of the heart as evidenced by displacement of myocardial tags. Note, however, that this motion is much more pronounced in the inferior wall where a greater step-off of the tag line can be seen (curved arrow). There is also twisting of some intramyocardial tag lines, especially in the inferior and left lateral wall (arrowheads), reflecting different degrees of twisting motion between subendocardial and subepicardial regions. Depiction of such intrinsic patterns of myocardial contraction have not been possible without invasive methods.

displacement of the tags in the stationary regions of the phantom was observed on successive acquisitions with and without motion.

The minimum angular displacement observed was 2°, with the phantom rotating at 0.2 revolutions per second, corresponding to a linear velocity of 7.5 cm per second at the periphery of the 12-cm-diameter phantom. No distortion of the phantom image was seen at this velocity.

At 0.2 revolutions per second, a series of images was obtained at increasing TDs after tagging to study angular displacements measured in degrees. This was done with the line defined by the center of the phantom and the imprint of the tag on the stationary regions of the phantom as reference, and the line defined by the displaced tag and the center of the phantom. Images with increasing TDs up to 450 msec, in 50-msec increments, demonstrated increasing angular displacement, and the measured values plotted against predicted values fit to a line, $\theta m = 0.95\ \theta p + 1.1$. The correlation coefficient was .98, and standard deviation was 2.8°.

In these preliminary experiments, a 128 × 128 matrix with pixel size of 1.8 × 1.8 mm was used to shorten imaging time requirements. With such large pixels, the inherent uncertainty of measurement is quite large, but finer image matrixes with longer acquisition times can easily be obtained for more accurate studies.

With human subjects, three tagging schemes were successfully implemented. In two subjects, two sets of three parallel 0.35-cm-thick tagging planes generated with two multifrequency RF pulses 12 msec apart in the short axis of the left ventricle were followed by five sequential 1-cm-thick long-axis images, each requiring 57 msec and equally distributed from 50 to 335 msec after tagging (Fig 4). The amount of translation of myocardium, measured as the distance between a given tag and its original position at diastole (determined by the line passing through the tags in the chest wall) was heterogeneous. Significantly greater basal than apical motion was demonstrated in these two subjects. When end-systolic images were used, the most basal tags translated toward the apex by an average of 1.7 cm ± 0.4. Tags located at a point midway between base and apex translated toward the apex by an average of 0.8 cm ± 0.3, and apical tags translated in a base-to-apex direction by 0.2 cm ± 0.2.

In one subject, a gridlike tagging pattern generated by two intersecting triple-frequency RF pulses was used (Fig 5). In the remaining five subjects, four radially distributed tagging planes were generated in 36 msec along the central long axis of the left ventricle and were followed after TDs of 0–550 msec by imaging in the short axis (Fig 6). This distribution of tags defines eight radial segments per section. Tags were clearly seen 50–450 msec after tagging in the myocardium but only 50–250 msec in the epicardial fat as a result of the shorter T1 of fat. As expected, tags were not recognizable in the ventricular cavity because velocity and turbulence of flowing blood rapidly destroys the integrity of the tags.

Angular displacement of the tags at end systole, measured relative to a reference line passing through the centroid of the left ventricular cavity and the imprint of the tag on stationary structures such as the chest wall, showed heterogeneous rotation with increasing degrees of clockwise rotation from base to apex of 0°–20°. Furthermore, differences in the degree of rotation of epicardial and endocardial points were demonstrated, implying a twisting motion during contraction of the ventricle. This twisting motion pattern was more pronounced at the apex. Differences in degrees of rotation and twist were also observed within segments of the same section with more motion in the posterolateral and inferior walls (Fig 6b, 6c). The preliminary nature of this study focused on demonstrating the technical feasibility of the method rather than on studying ventricular physiologic characteristics, and the limited number of subjects does not permit a firm interpretation of these data. However, it appears that the technique can demonstrate

differential motion between myocardial tissue layers heretofore not demonstrable without invasive markers. More experiments will be needed to fully quantify and validate these preliminary observations.

DISCUSSION

MR imaging is sensitive to motion within the tested object, and a great deal of effort has been directed to exploiting this property in the assessment of blood flow (7–10). Techniques of flow assessment with MR imaging rely on two generic methods of motion encoding, those based on phase shifts exhibited by resonant protons moving along magnetic-field gradients and those based on disturbing the magnetization, that is, tagging a portion of the sample and recording the passage of these partially saturated protons at a later time and in a different location, also known as time-of-flight methods.

The method presented in this report is akin to the tagging methods used for blood flow studies. In blood, turbulence and high velocity can scatter the perturbed protons and impair their recognition, whereas protons in heart muscle do not undergo dispersion, thus enabling recognition of the tags throughout the cardiac cycle. In addition, unlike phase-shift methods (11), tagging methods are totally independent of the direction of applied gradients, and any pattern of motion can be recorded. Since the pattern of motion of the myocardium during the cardiac cycle is complex and even in the normal heart involves displacement along all three coordinate axes, tagging methods should be well suited to such studies.

The major goal of this report is to demonstrate the feasibility of using MR imaging to overcome uncertainties in measuring diastolic-to-systolic events because of the absence of sufficiently distinctive anatomic ventricular landmarks that can be reliably tracked throughout the cardiac cycle. Currently, radiopaque metallic markers or in situ measurement devices such as microsonometers have to be used when more accurate measurements are sought (5,6). In humans, they can be placed only during clinically indicated surgery and in limited numbers. Even with the usual eight to ten markers, left ventricular mass and regional wall motion can only be approximated with crude model-reconstruction methods and arbitrary internal and external landmarks (4,12). The versatility and totally noninvasive nature of the method presented here should permit detailed studies of the normal and abnormal myocardium in both animals and humans with sufficient virtual RF markers, even in regions where physical markers or devices cannot easily be implanted, such as the ventricular septum. Variations of the basic method are limited only by the RF and gradient power-supply requirements of the equipment.

As demonstrated in human subjects, tag depiction was achieved to 450 msec at 0.38 T. Although this time is shorter than the average R-R interval, it is sufficient to study the contractile phase of the cardiac cycle. When necessary, tracking time can be lengthened to encompass the entire cardiac cycle by acquiring data at every second or third heartbeat, thus increasing effective TR. A unique advantage of the method is its ability to display myocardial twist occurring during contraction. In addition, more accurate assessment of geometric changes throughout contraction may be possible, since identical myocardial regions can be compared from diastole to systole. This may prove useful in reducing the large variability and poor reproducibility of measurements currently observed even between adjacent segments of the normal ventricle (13).

Obviously, further technical refinements and data validation are required before the exact impact of this method can be ascertained. ■

Acknowledgments: We thank Craig Barratt for providing us with expertise and software to generate the multifrequency RF pulses used in this project. We thank Myron Weisfeldt, MD, and James Weiss, MD, from the Division of Cardiology, and Renate Soulen, MD; Elliot McVeigh, PhD; and William Brody, MD, from the Department of Radiology, for thoughtful advice, criticism, support, and encouragement. Administrative and secretarial support was provided by Priscilla Mangum.

References

1. Borer JS, Bacharach SL, Green MV, Kent KM, Epstein SE, Johnston GS. Real-time radionuclide cineangiography in the noninvasive evaluation of global and regional left ventricular function at rest and during exercise in patients with coronary-artery disease. N Engl J Med 1977; 296:839–844.
2. Gallagher KP, Kumada T, Koziol JA, McKown MD, Kemper WS, Ross J. Significance of regional wall thickening abnormalities relative to transmural myocardial perfusion in anesthetized dogs. Circulation 1980; 62:1266–1274.
3. Lieberman AN, Weiss JL, Judgutt BI, et al. Two-dimensional echocardiography and infarct size: relationship of regional wall motion and thickening to the extent of myocardial infarction in the dog. Circulation 1981; 63:739–746.
4. Falsetti HL, Marcus ML, Kerber RE, Skorton DJ. Quantification of myocardial ischemia and infarction by left ventricular imaging. Circulation 1981; 63:747–751.
5. Ingels NB Jr, Daughters GT 2d, Stinson EB, Alderman EL. Evaluation of methods for quantifying left ventricular segmental wall motion in man using myocardial markers as a standard. Circulation 1980; 61:966–972.
6. Myers JH, Stirling MC, Choy M, Buda AJ, Gallagher KP. Direct measurement of inner and outer wall thickening dynamics with epicardial echocardiography. Circulation 1986; 74:164–172.
7. Carr HY, Purcell EM. Effects of diffusion on free precession in nuclear magnetic experiments. Phys Rev 1954; 94:630.
8. Singer JR. Blood flow rates by nuclear magnetic resonance measurements. Science 1959; 130:1652–1653.
9. Moran PR. A flow velocity zeugmatographic interlace for NMR imaging in humans. Magn Reson Imaging 1982; 1:197.
10. Axel L. Blood flow effects in magnetic resonance imaging. AJR 1984; 143:1157–1166.
11. Van Dijk P. Direct cardiac NMR imaging of heart wall and blood flow velocity. J Comput Assist Tomogr 1984; 8:429–436.
12. Altschule MD. Uncertainties in the interpretation of abnormal ventricular wall motion. Chest 1986; 89:749–750.
13. Pandian NG, Skorton DJ, Collins SM, Falsetti HL, Burke ER, Kerber RE. Heterogeneity of left ventricular segmental wall thickening and excursion in 2-dimensional echocardiograms of normal human subjects. Am J Cardiol 1983; 51:1667–1673.